IOPscience iopscience.iop.org

Home Search Collections Journals About Contact us My IOPscience

Neutron scattering material analysis of Bronze Age metal artefacts

This article has been downloaded from IOPscience. Please scroll down to see the full text article.

2008 J. Phys.: Condens. Matter 20 104253

(http://iopscience.iop.org/0953-8984/20/10/104253)

View the table of contents for this issue, or go to the journal homepage for more

Download details:
IP Address: 129.252.86.83
The article was downloaded on 29/05/2010 at 10:44

Please note that terms and conditions apply.

IOP Publishing | Journal of Physics: Condensed Matter

J. Phys.: Condens. Matter **20** (2008) 104253 (8pp) doi:10.1088/0953-8984/20/10/104253

Neutron scattering material analysis of Bronze Age metal artefacts

L Cartechini[1], R Arletti[2], R Rinaldi[3,5], W Kockelmann[4], S Giovannini[2] and A Cardarelli[2]

[1] ISTM-CNR, Perugia and Centro di Eccellenza SMAArt, Università di Perugia, Italy
[2] Dipartimento di Scienze della Terra Università di Modena e Reggio Emilia, Italy
[3] Dipartimento di Scienze della Terra and Centro di Eccellenza SMAArt, Università di Perugia, Italy
[4] Rutherford Appleton Laboratory, ISIS Facility, Chilton, Didcot, UK

E-mail: rrinaldi@unipg.it

Received 30 July 2007, in final form 21 September 2007
Published 19 February 2008
Online at stacks.iop.org/JPhysCM/20/104253

Abstract
Non-destructive characterization of bronze artefacts from archaeological finds of the 'Terramare' dwellings near Modena, Italy, was carried out by time-of-flight neutron scattering at the ISIS spallation neutron source of the Rutherford Appleton Laboratory, UK. This provides information on ancient metal technology and its development through the Bronze Age in that region. Six pieces from three different classes as to use and manufacture, from the Middle to Late Bronze Age, were investigated on the ROTAX and GEM beam lines at ISIS, providing a comparison between results from the two instruments. A comparison is also made with three axes of the same area of provenance (Emilia, Terramare culture) from the Early, Middle and Late Bronze Age respectively, analysed previously.

Data collected provide stable refinements of the phase fractions and lattice parameters by the Rietveld method, allowing determination of Sn contents from the unit cell expansion due to the incorporation of Sn into the Cu-type α-phase. Notably, two of the objects exhibit a range of Sn contents in the bulk as is evident from broad diffraction peaks (4–8 and 10–14 wt% Sn), while the other four artefacts have more defined Sn contents of 8, 9, 10 and 14.5 wt% respectively. The higher Sn weight fractions are associated with the presence of pure unalloyed Cu, interestingly coexisting in one case with two bronze phases (α and the eutectoid δ). One sample shows the presence of 2–3 wt% Pb. Varying amounts of oxidation products such as cuprite were identified. Texture information extracted from the diffraction data provided some indications of different working treatments of the analysed objects.

(Some figures in this article are in colour only in the electronic version)

1. Introduction

'Terramare' is the name given to archaeological sites characterized by patches of a peculiar dark rich soil (hence the name) marking the presence of Bronze-Age settlements built as artificially fortified villages which, between the 17th and the 12th century BC, were densely occupying the central part of the river Po plains in Northern Italy [1]. The economic success of the social and cultural model of these settlements determined a strong demographic growth associated with a large artisan production. From the thousands of finds of bronze artefacts and from the testimony of their local production, one can safely assume that already in these early times there were specialized artisans who destined a large proportion of their work to the production of goods for the community. In particular, the metallurgic production of bronze seems to have been most prominent and articulated. Together with arms (daggers and swords), many ornaments (pins, brooches, buckles, bracelets, etc) and work utensils (axes, sickles, scalpels, etc) have been found. Towards the end of this period, objects made of laminated metal also began to appear.

Such an articulated production implies a remarkable workmanship and the knowledge of many different working

[5] Author to whom any correspondence should be addressed.

 © 2008 IOP Publishing Ltd Printed in the UK

procedures depending on the type of object to be produced. For instance, the different tin content detected in different objects may be correlated with the use for which they were destined [2, 3]. However, understanding of these different working processes is at present severely limited by the fact that many of these objects are rather small (i.e. the ornaments) and totally unsuitable for invasive sampling procedures even at the micro-sampling level. Therefore the use of a totally non-destructive analytical method such as neutron diffraction is highly desirable if not mandatory in this case.

The aim is that of providing an otherwise unobtainable contribution to the knowledge of the metal alloy materials produced by the Terramare populations by analysing several bronze objects selected on the basis of their different purposes (arms, ornaments, utensils) to obtain significant results as to their fundamental properties and possible correlations between these and the different production procedures. The direct comparison among the various kinds of artefacts should also provide an archaeometric key for the reconstruction of this ancient technology.

It was recently demonstrated that compositional and microstructural data can be obtained on archaeological bronzes using time-of-flight neutron diffraction (TOF-ND) [4, 5]. It was also shown that on a TOF instrument reliable and quantitative information can be obtained from intact archaeological objects of almost any shape [4, 5]. The object is left undisturbed and the analysis is totally non-destructive. Furthermore, activation of bronze objects has typical decay times of 2 days for data collection times of 2–3 h. The neutron beam size is large enough (of the order of 1 cm^2) to probe large parts of an object, thus overcoming a major disadvantage of many conventional archaeometric methods, where small spot sampling and strongly absorbing samples (e.g. SEM, XRPD, μ-XRF [5, 6]) do not necessarily provide the characteristic material properties of the whole object.

Neutron scattering experiments are therefore well suited to provide the following.

(1) Quantitative determinations of the phases and of the Cu–Sn alloy compositions from lattice parameter measurements by assuming a Vegard-type unit cell expansion for the incorporation of Sn into the copper lattice.
(2) Quantitative information on inclusions (if present) and on the oxidation/alteration/deposit on the surface of or within the pieces. These phases, when capable of producing measurable signals, do not represent a significant encumbrance on the analysis of the bulk, unaltered, alloy material.
(3) Information on the manufacturing process the artefacts underwent from texture measurements through the determination of the orientation distribution of crystallites.

The combination of these analytical results, obtained in a non-destructive mode, may provide clues in order to discriminate among different working processes (alloying fusion, cold/hot working procedures, etc), and burial environment (alteration, corrosion, etc). Hence, it may be possible to establish the level of technology achieved in the various production centres and some indication as to the state of preservation and interventions necessary for an effective conservation of the artefacts.

2. Samples

We collected neutron diffraction data on six artefacts destined for different uses, and dating from different periods of the Bronze Age. Shapes and dimensions vary greatly according to the type of object but they are all in the hand-size range. The six pieces (figure 1) pertain to three different classes of objects, namely a sword blade fragment and a spear head (weapons; samples S. Ambrogio-72 and S. Ambrogio-5, respectively), two garment pins (ornaments; samples Redù-30 and Montale-255, respectively) and a sickle blade and a knife or dagger handle (tools; samples Gorzano-14 and Redù-8, respectively). Each class is represented by two artefacts from the same period. The total number of samples was dependent on beam-time availability. Although fairly representative, the number was certainly not redundant.

This work was undertaken in order to complete a previous exploratory study [7, 8] carried out on three axes of the same area of provenance (Emilia, Terramare culture) dating from the Early, Middle and Late Bronze Age respectively. We have thus expanded the scope of the research to a total number of artefacts representative of different utilizations in order to explore more systematically the diversity of metallurgical recipes involved in the production of objects pertaining to a variety of end uses.

3. Experimental details

Several spots of interest were examined on each sample on the ROTAX and GEM beam lines, according to dimensions and shape, with a neutron beam size varying in the range from 0.5×0.5 to 1×2 cm^2. Typical exposure times for data collection on ROTAX were about 1–2 h, as previously observed for the characterization of thin walled bronze objects [5, 6]. In the case of sample S. Ambrogio-5 (spear head) two measurements were carried out on the same spot with and without a Cd foil absorber placed inside the cavity of the piece which has a relatively small separation of 1–2 cm between the two walls. This eliminated broadening effects due to scattering contributions from the front-side and the back-side of the object.

Texture measurements are best carried out on GEM in the stationary mode, taking advantage of a multitude of detector orientations [8, 9]. Due to beam-time limitations, texture data were collected only on 1 or 2 parts of the object. Based on experience with previously studied archaeological bronzes, the interpretation of phase and texture analyses relied on the diffraction results obtained for bronze reference samples produced in the laboratory in a controlled way [10].

The quantitative determination of the phases is obtained by analysing both ROTAX and GEM diffraction patterns by a full-profile Rietveld refinement method [11] using the GSAS program [12] with the EXPGUI [13] interface. The analysis was carried out on the sum of spectra from all the detector

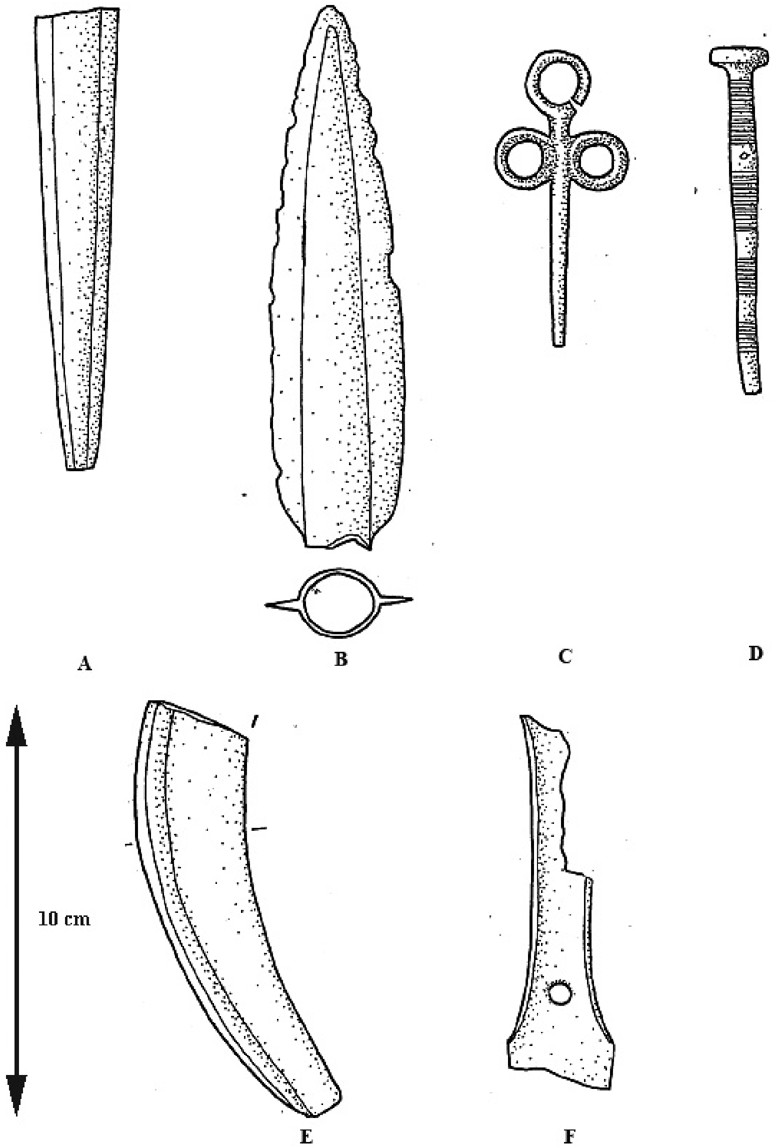

Figure 1. Top: middle Bronze Age. (A) S. Ambrogio-72 sword blade; (B) S. Ambrogio-5 spear head; (C) Redù-30 garment pin; (D) Montale-255 garment pin. Bottom: late Bronze Age. (E) Gorzano-14 sickle blade; (F) Redù-8 dagger handle.

elements of each bank of the two experimental lines. The data were normalized to the incident neutron flux distribution. ICSD and CrystMet databases [14, 15] were used as the source of the reference crystal structures (symmetry, space group, lattice parameters, atom positions). Phase analysis was carried out by refining one overall Debye–Waller parameter and one common absorption parameter for all patterns of the same analysis spot.

In the case of the bronze phase, a peak broadening parameter γ_1, derived from the Rietveld analysis assuming a pure Lorentzian broadening of the peak profiles, was used to calculate a parameter ε_γ, which provides a measure of the micro-strains induced in the crystallites by cold working of the metal object [7]. As a matter of fact, the information provided by the ε_γ parameter is only indicative, being based on a fairly coarse approximation and can be seen as an overall estimation of the broadening that also includes contributions from Sn variations and grain size effects. However, these values can be used with a certain degree of confidence to compare different analysis points on the same object or among different objects, and in comparison with values obtained from laboratory reference samples.

Copper/tin alloy compositions were obtained from measurements, by Rietveld refinement, of the α-bronze phase lattice parameters. This is based on the observation of a Vegard-type cell edge expansion for the fcc α-Cu phase (with corresponding shifts of the Bragg peaks) and its linear correlation with Sn wt% (estimated accuracy of ± 0.5 Sn wt%) found in alloys containing up to 14 wt% Sn, where formation of the alpha phase is dominant [10, 16]. For two samples diffraction profiles characterized by broad and structured bronze peaks were observed as a result of a strong heterogeneity of the alloy composition (as discussed in the following section). In these cases Rietveld refinement was carried out by assuming the presence of two bronze phases having copper/tin compositions corresponding to the lower and

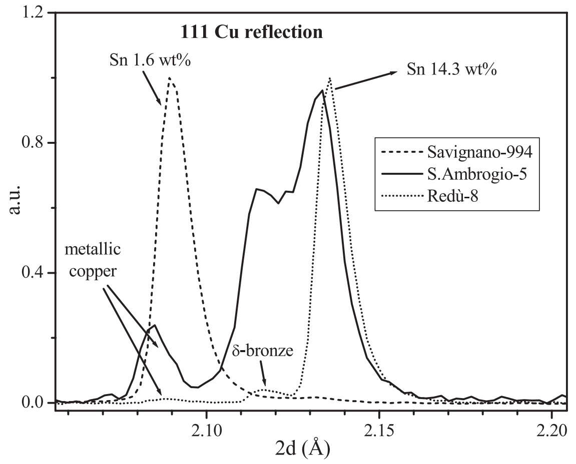

Figure 2. Comparison of the (111) Cu reflection profiles in three samples: Savignano-994 (axe—Early Bronze Age); S. Ambrogio-5 (spear head—Middle Bronze Age); Redù-8 (dagger handle—Late Bronze Age). The different Cu contents are responsible for peak *d*-spacing shifts. The highly structured peak profile for sample S. Ambrogio-5, reveals the presence of a wide range of compositions for the bronze alloy, including a considerable proportion of unalloyed Cu. Bronze alloy in sample Redù-8 shows the highest tin content combined with the presence of the delta phase and of minor amounts of unalloyed copper. Sample Savignano-994, by comparison, shows, with a much lower Sn content, the highest degree of homogeneity among the three.

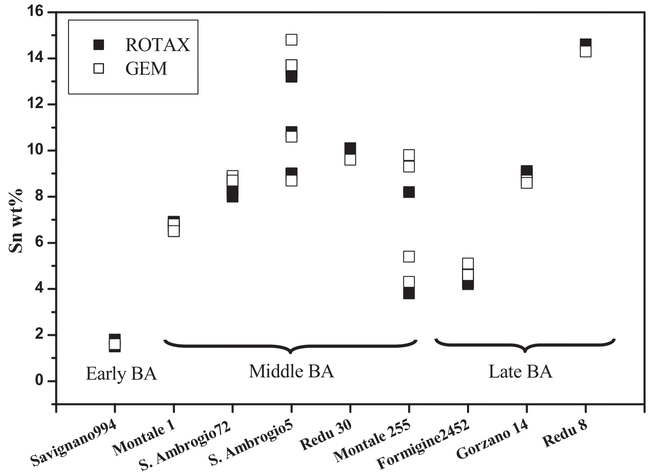

Figure 3. Alloy compositions (Sn wt%) are reported for all the points analysed for each sample at ROTAX and GEM beam lines. The three axes from previous works (Savignano-994, Montale-1 and Formigine-2452) are also included for comparison. For samples S. Ambrogio-5 and Montale-255, compositions corresponding to the lower and upper limits of the Sn wt% variation range are shown.

the upper limit of the range of variation. In the following tables an overall alpha-phase fraction is given as the sum of the two individual alpha-bronze phases. Evidently in this case the heterogeneity of the alloy prevented any strain analysis through the peak broadening parameter.

The bronzes are further characterized by the texture information obtained from the GEM measurements. Crystallographic texture in polycrystalline materials is defined as the non-random distribution of crystallites; this is reflected in a change of relative Bragg intensities in the diffraction profiles for different sample orientations with respect to the detector and the incident beam [17]. GEM provides for the simultaneous collection of data for many sample orientations; therefore, providing a wide coverage for the study of the orientation distribution function in a single measurement [8, 9]. The texture analysis program MAUD was used for extraction of the orientation distribution functions and reconstruction of complete pole figures [18]. In the case of the highly symmetrical fcc cubic crystal lattice of copper and bronze, the main crystallographic directions ⟨111⟩, ⟨200⟩, and ⟨220⟩ are normally used for pole figure representation. Such pole figures may often serve as fingerprints [4] and give a direct view of typical textural properties impressed on metal artefacts by working treatments such as hammering, rolling, and casting.

4. Results and discussion

4.1. Composition

The study of the six samples from Middle to Late Bronze Age revealed a more complex situation than that of the three axes previously examined [7, 8], with a larger variability in the alloy composition, higher tin contents (up to 14% Sn) and distinct compositional heterogeneities in some of the samples, as revealed by some highly structured peak profiles in the diffraction patterns. An example is reported in figure 2, where the (111) reflection reveals different alloy compositions and different degrees of homogeneity for three of the samples taken for comparison (Savignano-994 axe, Early Bronze Age; S. Ambrogio-5 spear head, Middle BA; Redù-8 dagger handle, Late BA). Figure 2 also shows that the diffraction resolution on ROTAX and GEM is able to resolve pattern profile features for bronze alloys having compositional differences as low as 0.5 Sn wt%.

The compositional differences and the various degrees of homogeneity of the alloys can lead to a variety of interpretations and conclusions in terms of their archaeological significance, which are outside the scope of this work as they have to draw from a much wider context of information. However, it seems appropriate to note here that the least refined metal smelting technology seems to be associated with less durable objects, such as the head of a projectile weapon (S. Ambrogio-5 spear head).

Tables 1 and 2 report the results obtained from Rietveld refinements of ROTAX and GEM data respectively, showing good agreement between the two sets of measurements. Small differences can be attributed to slight variations of the analysis spot position. Figure 3 shows a plot of the results in terms of Sn alloy compositions for all the pieces analysed from Terramare sites, including the three axes from previous works for comparison.

Four samples (S. Ambrogio-72 sword blade; Redù-30 garment pin; Gorzano-14 sickle blade: Redù-8 dagger handle) have rather homogeneous α-bronze compositions, showing tin fractions of about 8, 9, 10 and 14.5 wt% respectively, with standard deviations of the order of 1%, resulting, in figure 3,

Table 1. Line broadening analysis (ε_γ), alloy composition (Sn wt%) and phase analysis (wt%) from ROTAX data.

Sample	Strain parameter	Bronze composition (estimated error ±0.5 wt%)	Phase analysis wt% (estimated error ± 0.2wt%)			
S. Ambrogio-72 (middle BA)	ε_γ	wt% Sn	α bronze			
0 mm (blade)	0.49	8.2	100.0			
5 mm	0.32	8.4	100.0			
9 mm	0.36	8.0	100.0			
18 mm	0.29	8.8	100.0			
S. Ambrogio-5 (middle BA)	ε_γ	wt% Sn	α bronze	Cu	Cu_2O	Calcite
P1 body	—	9.0–13.2	94.0	5.1	0.8	—
P1 body[a]	—	10.8–13.7	96.8	2.8	—	0.4
P2 body[a]	—	9.0–13.4	90.3	7.8	—	1.9
P3 spearhead[a]	—	9.0–13.5	99.2	0.5	—	0.3
Redù 30 (middle BA)	ε_γ	wt% Sn	α bronze	Cu_2O		
Body	—	10.1	95.7	4.3		
Montale-255 (middle BA)	ε_γ	wt% Sn	α bronze	Cu_2O	Pb	
Body	—	3.8–8.2	89.1	8.2	2.8	
Gorzano-14 (late BA)	ε_γ	wt% Sn	α bronze	Cu_2O	Nantokite	
5 mm (back)	0.17	9.1	97.4	2.3	0.3	
10 mm (centre)	0.15	9.0	95.2	4.2	0.6	
25 mm (blade)	0.48	9.1	97.2	2.8	—	
Redù 8 (late BA)	ε_γ	wt% Sn	α bronze	δ bronze	Copper	Cu_2O
Body	0.00	14.6	88.2	4.9	1.4	5.4

[a] Cd foil inside.

Table 2. Line broadening analysis (ε_γ), alloy composition (Sn wt%) and phase analysis (wt%) from GEM data.

Sample	Strain parameter	Bronze composition (estimated error ±0.5 wt%)	Phase analysis wt% (estimated error ±0.2 wt%)				
S. Ambrogio-72 (middle BA)	ε_γ	wt% Sn	α bronze	Chalcocite			
Blade	0.45	8.9	100.0	—			
Body	0.39	8.7	99.1	0.9			
S. Ambrogio-5 (middle BA)	ε_γ	wt% Sn	Bronze	Cu	Cu_2O	Calcite	Quartz
Body	—	8.7–13.7	76.8	10.8	4.5	5.6	2.2
Blade	—	10.6–14.8	66.8	26.6	5.7	0.3	0.6
Redù 30 (middle BA)	ε_γ	wt% Sn	α bronze	Cu_2O			
Body	0.69	9.6	93.1	6.9			
Montale-255 (middle BA)	ε_γ	wt% Sn	α bronze	Cu_2O	Pb		
Body	—	5.4–9.8	88.1	9.7	2.2		
Head	—	4.3–9.3	90.1	8.0	1.9		
Gorzano-14 (late BA)	ε_γ	wt% Sn	α bronze	Cu_2O	Nantokite		
Back	0.23	8.7	91.0	8.8	0.2		
Blade	0.48	8.6	90.7	8.8	0.5		
Redù 8 (late BA)	ε_γ	wt% Sn	α bronze	δ bronze	Copper	Cu_2O	
Body	0.00	14.3	85.9	13.3	0.2	0.6	

in tight clusters of the experimental points. In the case of the inhomogeneous samples S. Ambrogio-5 (spear head) and Montale-255 (garment pin), alloy compositions varied in the ranges of 10–14 Sn wt% and 4–8 Sn wt%, respectively, as shown in figure 3 by a significant spread of the Sn wt% values. Such Sn/Cu segregation effects are usually observed in cast materials which did not have enough time to homogenize during cooling and implicate the lack of high temperature annealing treatments of the pieces [19]. Due to the high degree of broadening and to the presence of deeply structured peaks (see figure 2), line width analyses were not possible for these two samples.

The observed large variability of alloy composition among all the objects examined shows no direct relation between tin content and age. Notably, the oldest axe (early BA) has the lowest amount of Sn, possibly an indication of the scarcity of this element at the onset of this metallurgical technique. Furthermore, samples pertaining to the same typology of objects (i.e. garment pins) also show different alloy compositions and homogeneity, providing a challenge for an archaeological explanation. Nevertheless, it seems as though the effect of tin content on the mechanical properties of the metal might have been an established knowledge, the tin content being kept below 14 wt% for all objects with the sole exception of sample Redù-8, which exhibits a high-tin bronze phase. As a matter of fact, alloy compositions in the range 8–10 Sn wt% are characterized by the best mechanical properties related to resistance and workability of the metal, while with tin contents higher than 14% the eutectoid delta bronze phase may form [19]. This phase is hard and brittle and hinders workability of the piece. This is the case of sample Redù-8, the dagger handle, where the presence of the delta phase may be accidental but it is not in contrast with the making of a sharp blade.

These observations confirm that the Terramare metallurgic production was varied and complex, showing a high level of technological evolution.

With regards to the use of lead in alloy manufacture, the Pb content of about 2 wt% found in garment pin Montale-255 may hint at a search for ease of casting. No evidence of lead inclusions was found in the other pieces. Notably, similar Pb concentrations were observed in the late and middle Bronze Age axes.

Considering the phase analysis results in tables 1 and 2, almost all the samples show a good state of preservation. As expected, the presence of cuprite (Cu_2O) as the main alteration product (and/or formation during casting) is confirmed for almost all samples. Only one sample shows a poorer state of preservation, as evidenced by the presence of nantokite (CuCl), a sure sign of degradation of the metal [19]. Chalcocite (Cu_2S) was observed only in sample S. Ambrogio-72, and it may originate from residues of sulfide copper ore used for alloy production. Finally, calcite and quartz derive from residues of the burial materials or clay core material still present in the inner part of the hollow piece (S. Ambrogio-5).

Furthermore, phase analyses for different spots on the same object show variable compositions, suggesting a marked heterogeneity of alteration and patina layers. This is in agreement with the general observation of a highly localized and specific nature of corrosion/alteration phenomena in metal artifacts.

An interesting result from the phase analysis is also the detection of unalloyed copper inclusions (UCIs) in two of the pieces with the highest tin contents (13–14 wt%). These inclusions open an array of questions related to their origin. In the literature there are many examples of ancient bronzes showing unalloyed copper inclusions [20]. Three different main sources have been proposed.

(1) Incomplete mixing of the metals during casting (the simplest mechanism).
(2) Tin-rich alloys with $\alpha+\delta$ eutectoid. It has been established that tin-rich phases are preferentially corroded in low oxygen environment as occurs for the inner part of the object. The corrosion may occur by destannification or by removal of all the delta eutectoid phase followed by Cu redeposition in the interdendritic spaces. Both situations have been observed in metallographic analyses on bronzes having the same provenance as ours [20].
(3) UCIs have been observed in the presence of copper sulfides as copper-rich spherical particles coated with a copper sulfide layer. They are formed during roasting of the mineral before alloying and casting.

For sample Redù-8 the second type of model is consistent with the experimental observations where a tin-rich alpha phase (Sn wt% above 14) is quite homogeneous and copper inclusions are observed in the presence of the delta phase eutectoid. The latter begins to appear between 5 and 15% Sn depending on cooling [21]. In this compositional range it can be eliminated by annealing, hence its presence hints at the lack of substantial heat treatments of the piece.

For sample S. Ambrogio-5 both (1) and (2) are possible. The heterogeneous character of the alloy with variable tin contents may indicate the occurrence of an incomplete mixing of Sn in Cu. However, we cannot exclude the presence of the delta phase because of the overlapping with the alpha phase with Sn contents of about 11 wt% which is present in the alloy. Mechanism (3) can be excluded for both samples since no evidence of copper sulfide inclusions was observed with the unalloyed copper. Tin-containing alteration products have not been detected, possibly due to their small amount, below the detection limit of the technique. Alternatively, amorphous tin compounds may be formed in the corrosion layer [22] not detectable by the diffraction technique. It should be noted that neutron diffraction cannot show the presence of small amounts of alloying elements, other than tin, such as arsenic or antimony, in solution in the copper lattice. The current analysis assumes that there is solely tin solved in the copper lattice to form bronze, and that the UCI phase consists purely of copper. The presence of other elements needs to be checked by a non-destructive elemental analysis method such as XRF or PGAA (prompt gamma activation analysis).

4.2. Strain and texture

ROTAX and GEM data were analysed for line broadening effects and texture properties of the samples with homogeneous alloys. We observed strain effects ($\varepsilon_\gamma \neq 0$) for all samples except Redù-8, which gives a null value for the ε_γ parameter. The object consists of the bulk portion of a dagger handle, which, presumably, was obtained as a cast piece for which the absence of any significant peak broadening excludes any substantial cold working treatment as the final working step, but at the same time indicates either a slow cooling rate or some significant heat treatment, which led to the homogenization of the alpha-bronze phase. At 14.6 wt%, the alpha phase is at its practical limit for the uptake of Sn. Hence, there is some

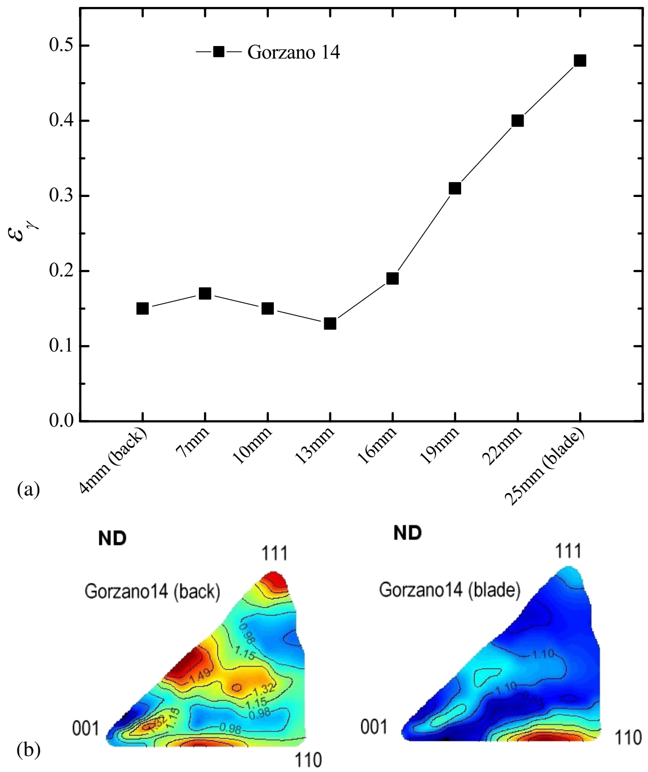

Figure 4. (a) ε_{γ} values for sample Gorzano-14 (sickle blade) collected at ROTAX by scanning the object in steps of 3 mm across the width of the blade. (b) Inverse pole figures of the 'normal direction' (N) obtained from GEM diffraction data collected in the centre (left) and on the blade (right) for sample Gorzano-14. Pole densities for the blade are concentrated around the (110) direction as expected for compression (hammering) texture of an fcc-metal.

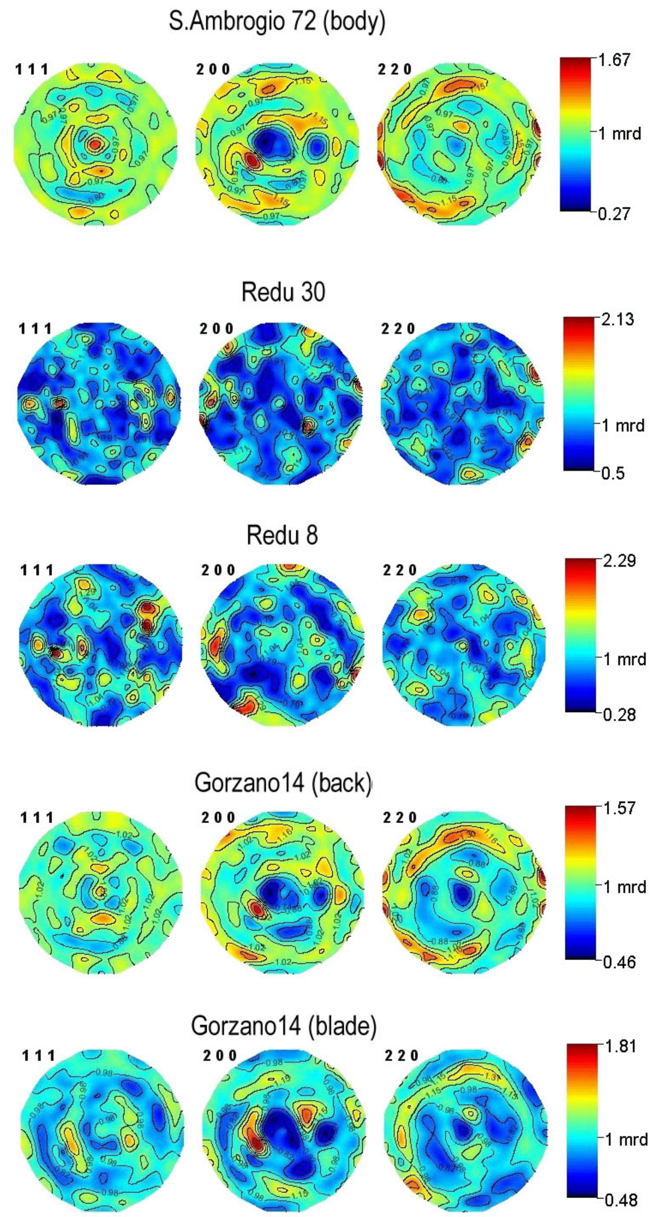

Figure 5. (111), (200) and (220) pole figures for Terramare bronze objects. The normal direction (perpendicular to the flat side of the object, see figure 1) coincides with the incident neutron beam direction in the centre of a pole figure.

considerable portion of the Cu–Sn delta phase present, i.e. the alloy is only partially homogenized.

In the case of samples S. Ambrogio-72 (sword blade) and Gorzano-14 (sickle blade), the higher values of ε_{γ} (0.45–0.49) correspond to the blade edges, where shaping work was probably applied in order to obtain cutting edges as sharp as possible. This was clearly shown by the results of the line width analysis carried out on diffraction data on several spots collected in a line across the width of the objects (from body to blade). We found a clear trend in the ε_{γ} values with an increase of the broadening effect from the body to the blade. Results for sample Gorzano-14 (sickle blade), collected by scanning the object in steps of 3 mm and with short acquisition times, are reported in figure 4(a). As expected, the broadening effect is smaller at the central part of the piece, where, presumably, shaping work was less pronounced than on the blade and on the back of the tool. The measured ε_{γ} values for these blades are slightly larger than those found in the previous study for the blades of the axes, characterized by thicker edges with rounded and smoother surfaces (ε_{γ} range: 0.15–0.43).

On the basis of the strain parameter results, texture analysis was considered in order to assess the presence of typical signatures of cold working treatments of the blades of the pieces. As a matter of fact, all textures observed are rather weak; i.e., only weak evidence of significant regular texture was found in the observed and recalculated pole figures.

Figure 5 displays pole figures of several of the objects. The observed textures are either rather irregular (Redu 8, Redu-30) or with slight indications of regular textures (S. Ambrogio-72, Gorzano-14) with maximum pole densities between 1.6 and 2.3 mrd (multiples of a random distribution). The textures of the latter objects are very similar, indicating some but not extensive application of cold treatment to produce sharp edges. These were instead produced by a shaping treatment, possibly the result of simple sharpening with a stone. The inverse and reconstructed pole figures for the Gorzano-14 piece are slightly different for back and blade (figures 4(b) and 5) with regard to the intensity and distribution of pole density maxima. The pole figures from the blade display pole densities more concentrated around the (110) direction, as expected of a piece that was hammered. This agrees with the elevated ε_γ values on the blade.

Samples Redù-8 and Redù-30 represent different, irregular textures typical of cast objects that have not seen any significant cold working treatment, but have suffered a different amount of heat treatment. Redù-8 displays a low ε_γ value, in agreement with a slow cooling or careful heat treatment. Redù-30 shows an anomalous high ε_γ value of 0.69 as determined by GEM data analysis, indicating rapid cooling or absence of heat treatment. The high ε_γ value and the irregular peak shape, indicating a dendritic structure of a cast with a range of Sn contents, suggest that Redù-30 has been left as cast, without significant homogenization treatment. It can be noted that the Rietveld refinement of the ROTAX data was complicated by an irregular spread of the scattering intensities over the detector channels due to the presence of large grains producing quite an irregular texture. The GEM data, being more randomized for the purpose of the phase analysis thanks to the larger detector coverage, provide more reliable structure and phase analysis results.

5. Conclusions

The results obtained in this study consist of the accurate determination of the bronze alloy composition and of the inclusions, corrosion and alteration phases for each of the objects examined. These results, combined with the analysis of micro-strain and texture, provide insights as to the manufacturing techniques, from the production of the alloy to the finishing treatments. An evaluation of the state of conservation is also achieved through the quantification of corrosion and alteration products.

The aim is that of providing the archaeologists with quantitative and qualitative measurements of fundamental properties of the materials used to produce the artefacts and of their transformation products. The objective information thus obtained finds its use in the context of all other observations in order to better define the socio-cultural environment and technological knowledge of the ancient populations under study.

The use of neutron diffraction has again proved to be particularly suitable for the non-destructive investigation of bronze artefacts. The technique in itself can provide complementary information to more traditional high resolution and high sensitivity material analysis techniques. However, in this case, where non-destructiveness is of paramount importance, it has allowed the systematic study and comparison of the material and manufacturing properties for a representative number of samples in a totally non-invasive approach preserving the absolute integrity of unique pieces.

Acknowledgments

Financial support is acknowledged from the Italian Ministry of Education (MIUR) for grant No 2004041033_4 (PRIN) to the Universities of Perugia and Modena and from NMI3 though FP6 (ISIS) to RR. We thank CNR for access to the ISIS Facility through the mutual agreement (No 01/9001) between CNR and CCLRC. The 'Centre of Excellence for Scientific Methodologies Applied to Archaeology and Art' (SMAArt) of Perugia University is also acknowledged for support. The Museo Civico Archeologico Etnologico of Modena is acknowledged for making this study possible.

References

[1] Carancini G L 1997 *Le Terramare: La più antica civiltà Padana* ed M Bernabò Brea, A Cardarelli and M Cremaschi (Milano: Electa) pp 379–404

[2] Giardino C 1998 *I metalli nel mondo antico. Introduzione all'archeometallurgia* (Roma-Bari: Laterza)

[3] Garagnani G L, Imbeni V and Martini C 1997 *Le Terramare: La più antica civiltà Padana* ed M Bernabò Brea, A Cardarelli and M Cremaschi (Milano: Electa) pp 554–66

[4] Kockelmann W, Siano S, Bartoli L, Visser D, Hallebeek P, Traum R, Linke R, Schreiner M and Kirfel A 2006 *Appl. Phys.* A **83** 175–82

[5] Cartechini L, Rinaldi R, Kockelmann W, Bonamore S, Manconi D, Borgia I, Rocchi P, Brunetti B G and Sgamellotti A 2006 *Appl. Phys.* A **83** 631–6

[6] Rinaldi R, Cartechini L, Kockelmann W, Bonamore S, Sgamellotti A and Brunetti B 2005 *Atti del III Congresso Nazionale di Archeometria* pp 329–39 Bressanone, Pàtron Editore, Bologna, ISBN 88-555-2832-7

[7] Arletti R, Cartechini L, Giovannini S, Rinaldi R, Kockelmann W and Cardarelli A 2007 *Nuovo Cimento* C **30** 11–9

[8] Arletti R, Cartechini L, Giovannini S, Rinaldi R, Kockelmann W and Cardarelli A 2007 Texture analysis of Bronze age axes by neutron diffraction *Appl. Phys.* A 1–6 at press (doi:10.1007/s00339-007-4225-0)

[9] Kockelmann W, Chapon L C and Radaelli P G 2006 *Physica* B **385/386** 639–43

[10] Siano S, Bartoli L, Zoppi M, Kockelmann W, Dayamond M, Dann J A, Garagnani M G and Miccio M 2003 *Proc. Int. Conf. on Archaeometallurgy in Europe* vol 2 (Milano: Associazione Italiana di Metallurgia) pp 19–29

[11] Young R A (ed) 1993 *The Rietveld Method* vol 5 (International Union of Crystallography, Oxford University Press)

[12] Larson A C and Von Dreele R B 1986 *GSAS: General Structure Analysis System Report, LAUR 86-748* Los Alamos National Laboratories, USA http://www.ccp14.ac.uk

[13] Toby B H 2001 *J. Appl. Crystallogr.* **34** 210

[14] 2004 *ICSD, Inorganic Crystal Structure Database* Germany & National Institute of Standards and Technology, USA http://www.fiz-informationsdienste.de/en/DB/icsd/index.html

[15] 2002 *CRYSTMET, Materials Toolkit 2.0.1* Toth Information Systems Inc. http://www.tothcanada.com/databases.htm

[16] Sidot E, Kahn-Harari A, Cesari E and Robbiola L 2005 *Mater. Sci. Eng.* A **393** 147–56

[17] Wenk H R and Van Houtte P 2004 *Rep. Prog. Phys.* **67** 1367–428

[18] Lutterotti L 2005/2007 *MAUD, Material Analysis Using Diffraction* www.ing.unitn.it/∼maud/

[19] Scott D A 2002 *Copper and Bronze in Art—Corrosion, Colorants, Conservation* ed Getty Conservation Institute (Los Angeles: Getty Trust Publication)

[20] Bosi C, Garagnani G L, Imbeni V, Martini C, Mazzeo R and Poli G 2002 *J. Mater. Sci.* **37** 4285–98

[21] Scott D A 1991 *Metallography and Microstructure of Ancient and Historic Metals* ed Getty Conservation Institute (Los Angeles: Getty Trust Publication)

[22] Robbiola L, Blengino J M and Fiaud C 1998 *Corros. Sci.* **39** 2083–111